^{31}P electron-nuclear double resonance of the P_{In} antisite in InP:Zn detected via luminescence

H. C. Crookham and T. A. Kennedy
Naval Research Laboratory, Washington, D.C. 20375

D. J. Treacy
United States Naval Academy, Annapolis, Maryland 21402
(Received 6 December 1991)

Optically detected electron-nuclear double resonance (ODENDOR) has been observed via photoluminescence from the first-neighbor ^{31}P shell of the phosphorus antisite in zinc-doped InP. Analysis of the ENDOR data confirms a tetrahedral arrangement of ^{31}P nuclei. The hyperfine interaction for each of these nuclei is axial with $|A_{\parallel}|/h = 368.0 \pm 0.5$ MHz and $|A_{\perp}|/h = 247.8 \pm 0.5$ MHz. These parameters are slightly different from those reported by Jeon *et al.* [Phys. Rev. B **36**, 1324 (1987)]. A shift of the ENDOR frequencies correlated with a change in the central nuclear-spin state has also been observed. We have been able to account for this shift with a perturbation treatment in which the electronic spin and central nuclear spin are treated exactly and a neighboring nuclear spin provides the perturbation. The best ENDOR signals are obtained with low optical-excitation-power density (~ 0.1 W/cm^2) and low microwave modulation frequency (17 Hz). These conditions emphasize the contributions to the optically detected magnetic-resonance signal from distant donor-acceptor pairs.

INTRODUCTION

Several studies have demonstrated that optically detected electron-nuclear double resonance (ODENDOR) can be a powerful tool for obtaining detailed structural information about defect sites in III-V semiconductors.[1-5] In a recent study on InP, Jeon *et al.* employed magnetic circular dichroism (MCD) ODENDOR, in which magnetic resonance on a paramagnetic ground state is detected through changes in an optical-absorption process. In that study, Jeon *et al.* examined the P_{In} antisite in InP.[2] They observed ENDOR transitions from the four nearest-neighbor ^{31}P nuclei as well as from the ^{113}In and ^{115}In in the second-nearest-neighbor shell.

If a paramagnetic state of the defect is not populated, MCD optically-detected-magnetic-resonance (ODMR) techniques are not possible. However, ENDOR can also be detected through changes in the luminescence from a paramagnetic excited state.[6,7] An ODENDOR transition assigned to the second-neighbor indium shell detected through photoluminescence (PL) has been reported.[8] However, detection of the ^{31}P lines have not been reported. Generally, ODMR lines detected via photoluminescence from donor-acceptor-pair (DAP) recombination are broadened by a donor-acceptor exchange interaction, which is very sensitive to the DAP separation. Difficulties in observing ENDOR transitions through photoluminescence from DAP recombination may also result from a broadening by donor-acceptor exchange interactions.[9]

In this paper, we report the observation of PL-ODENDOR lines from the nearest-neighbor ^{31}P nuclei of the P_{In} antisite. The hyperfine parameters derived from these data are slightly different from the ^{31}P nearest-neighbor hyperfine parameters reported by Jeon *et al.*[2] The dependence of these signals on a number of experimental parameters, including modulation frequency, rf power, microwave power, and laser power, were investigated. The best ENDOR signals were obtained under conditions which emphasize the contribution from distant donor-acceptor pairs. Thus, the ENDOR may stem from distant donor-acceptor pairs for which exchange interactions are quite small.

EXPERIMENTAL

The experiments were performed on a *K*-band (24 GHz) ODMR spectrometer operated in the Voigt geometry. The samples were excited with either a Kr-ion laser (Spectra-Physics, 165) or a 3-mW He-Ne laser (Aerotech, LSR2R). The best results were obtained by exciting the sample with the He-Ne laser. The laser output was filtered with an infrared-absorbing filter, and neutral density filters were employed to vary the excitation power. The best signal-to-noise ratio was obtained with an excitation power density between 0.05 and 0.1 W/cm^2. Luminescence was detected with a North Coast 817S Ge detector. The detector was preceded by either a 1.0-μm-long pass filter or a 1.3-μm-long pass filter. A 50-mW Gunn oscillator was used as the microwave source, and the microwaves were amplitude modulated with a *p-i-n* diode switch. The microwave cavity was modified to accommodate a two-turn rf coil. An rf signal to the coil was supplied by a Wavetek (model 2410) frequency synthesizer amplified by an ENI 550L amplifier. The rf power applied to the coil was typically 12–25 W.

In the ENDOR experiment, the magnetic field was fixed at a value which satisfies the electron-paramagnetic-resonance condition. Next, the radiofrequency was swept by stepping the synthesizer frequency by means of a general purpose interface bus (GPIB) with a microcomputer. The ENDOR signal was obtained through a lock-in amplifier, which measured changes in luminescence intensity synchronous with the microwave modulation as the radiofrequency was swept.

The sample used in this study was a Zn-doped liquid-encapsulated-Czochralski (LEC) grown, single crystal of InP (Naval Research Lab sample 2-74-H). The sample has a hole concentration at room temperature on the order of 10^{16} cm^{-3}.

RESULTS AND ANALYSIS

All of the ODMR and ODENDOR spectra were obtained by monitoring the deep PL band at 0.8 eV. The ODMR spectrum of the P_{In} antisite in InP in this sample has been reported previously.[10,11] In the present experiments, an isotropic spectrum consisting of two broad peaks [35.6 mT full width at half maximum (FWHM)], centered at 851.8 mT and split by 104.0 mT, was observed at a microwave frequency of 23.895 GHz. The g value ($g = 2.004 \pm 0.004$) and central ^{31}P hyperfine coupling constant ($A_0/hc = 0.097 \pm 0.003$ cm^{-1}) are in good agreement with previously published values.[10]

The ENDOR signal amplitude was found to be extremely dependent on the modulation frequency. Figure 1 shows ENDOR spectra taken at microwave modulation frequencies of 77, 35, and 17 Hz, which demonstrate the sharp increase in signal as the modulation frequency is decreased. At frequencies much above 77 Hz, the signals become very weak and difficult to observe. The signal amplitude does not increase significantly below 17 Hz.

Similarly, the ENDOR signal increased in intensity as the rf power applied to the coil was increased up to about 25 W. Above this power level, the ENDOR signal remained relatively constant while base line anomalies not due to magnetic resonance increased. The ENDOR linewidths showed no significant change as a function of rf power.

ENDOR spectra were recorded at several orientations in the $(01\bar{1})$ plane, with the magnetic field set to the center of the low-field ODMR peak and with the field set to the center of the high-field peak. The positions of ENDOR peaks at 810 mT (low-field ODMR line) are represented by asterisks in Fig. 2. Peak positions at 910 mT (high-field ODMR line) are shown as circles. Each of the peaks observed had a linewidth of approximately 1.2 MHz (FWHM). In changing the magnetic field from 810 to 910 mT a nearly isotropic shift in the frequency of each ENDOR peak by approximately 3.1 MHz was observed. This shift is much larger than the 1.723-MHz change expected to accompany a 0.1-T field shift due to the change in the ^{31}P nuclear Larmor frequency. Further investigation revealed that as the field is changed within the high-field ODMR line, the ENDOR peaks shift with a slope of 17.5 ± 0.7 MHz/T, showing the resonance to be from ^{31}P. A broad (2.5-MHz FWHM) ENDOR resonance attributed to the second-neighbor indium shell was observed at 19.2 MHz with a field of 810 mT.

The orientation dependence of the ENDOR peaks was simulated by a perturbation treatment of the following spin Hamiltonian:

$$\hat{\mathcal{H}} = \hat{\mathcal{H}}_0 + \hat{\mathcal{H}}_1 ,$$
$$\hat{\mathcal{H}}_0 = \mu_e \mathbf{S}\cdot\mathbf{B} + a_0 \mathbf{I}_0\cdot\mathbf{S} - \mu_n \mathbf{I}_0\cdot\mathbf{B} , \tag{1}$$
$$\hat{\mathcal{H}}_1 = \sum_{l=1}^{4} (\mathbf{I}_l\cdot\overleftrightarrow{\mathbf{A}}_l\cdot\mathbf{S} - \mu_n \mathbf{I}_l\cdot\mathbf{B}) .$$

In this procedure the terms involving the nearest-

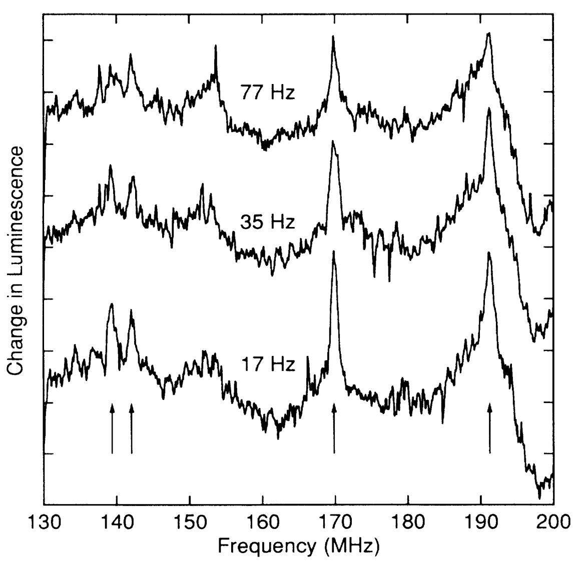

FIG. 1. Modulation frequency dependence of the ODENDOR signal. The experimental conditions were microwave power =50 mW, rf amplifier output =25 W, microwave frequency =23.895 GHz, and magnetic field =900 mT oriented 10° from [011] in the $(01\bar{1})$ plane. $T = 1.6$ K.

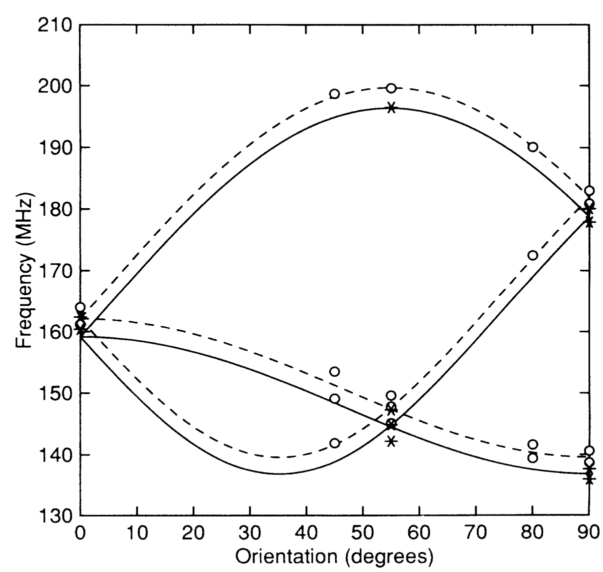

FIG. 2. Orientation dependence of the ^{31}P ENDOR lines for a rotation in the $(01\bar{1})$ plane where 0°≡[100] and 90°≡[011]. Asterisks are experimental peak positions at 810 mT. Open circles are peak positions at 910 mT. The solid curves and dashed curves are fits to the experimental points using the Hamiltonian parameters: $a_0 = 2.908$ GHz, $A_{\parallel} = 368.0$ MHz, $A_{\perp} = 247.8$ MHz.

neighbor nuclei ($\mathcal{H}_1$) were treated as a perturbation on zeroth-order states obtained by diagonalizing the terms which incorporate only the electron and central nuclear spins ($\mathcal{H}_0$). The perturbation treatment was carried to second order. A pseudo-dipole-dipole interaction between the nearest-neighbor nuclei, which becomes important at orientations where two or more nuclei are equivalent with respect to the magnetic-field direction, was not included in this calculation. This effect was explored thoroughly in the MCD-ODENDOR of InP by Jeon and co-workers.[2,12] They showed that in cases where nuclei are equivalent, this interaction has the effect of splitting the ENDOR lines symmetrically about the frequency calculated when the interaction is neglected. Therefore, the proper hyperfine parameter can be obtained by neglecting the pseudo-dipole-dipole interaction and fitting the average position of pseudodipolar split peaks. The solid and dashed lines in Fig. 2 are fits of the orientation dependence at 810 and 910 mT, respectively. The analysis confirms a tetrahedral arrangement of the nearest-neighbor nuclei, each with an axial hyperfine interaction. The hyperfine parameters were determined to be $|A_{\parallel}|/h=368.0\pm0.5$ MHz and $|A_{\perp}|/h=247.8\pm0.5$ MHz. $A_{\parallel}$, $A_{\perp}$, and the central hyperfine constant all have the same sign. Jeon *et al.* reported an $|A_{\parallel}|/h$ of 367.3 ± 0.2 MHz and an $|A_{\perp}|/h$ of 244.3 ± 0.2 MHz.

The analysis also shows that all of the observed ENDOR transitions arise from a single electron-spin manifold. For each of the observed ^{31}P ENDOR peaks, a second peak is expected approximately 30 MHz lower than the observed peak. No such peaks were detected.

DISCUSSION AND CONCLUSIONS

The unusually large shifts in the ENDOR frequencies between spectra taken on the low-field and high-field ODMR lines can be understood by considering the perturbation treatment of the spin Hamiltonian given by Eq. (1). This Hamiltonian is appropriate for a fixed acceptor spin state. For simplicity, only one nearest-neighbor nuclear spin is included. Figure 3 depicts the energy levels associated with the simplified Hamiltonian. In this case, the acceptor spin is chosen such that the levels in the upper electron-spin manifold are DAP states with short radiative lifetimes, and the levels of the lower manifold are DAP states with long radiative lifetimes. If the short-lifetime DAP states decay rapidly on the time scale at which nuclear-spin transitions can be induced, then ENDOR transitions will not be observed from these DAP levels. Therefore, ENDOR transitions can only be observed from the lower electron-spin manifold for this particular acceptor spin state.

In Fig. 3, the high-field ODMR transition is indicated by the thick arrow labeled (1). The thin arrow labeled (4) represents the ENDOR transition observed on ODMR transition (1). Likewise, transition (2) represents the low-field ODMR transition and transition (3) is the associated ENDOR transition. For the P_{In} case at 24 GHz, the large central hyperfine interaction produces a small but significant mixing of the electron-spin-central nuclear-spin Zeeman states. The appropriate eigenstates of $\mathcal{H}_0$ are indicated on the left side of Fig. 3. Consequently, the electron-spin states employed in the perturbation analysis for the energy levels involved in transition (3) are perturbed, but the electron-spin states used for transition (4) are pure. The use of different electron-spin states results in an approximately 1% (1.3-MHz) difference in the frequencies for transitions (3) and (4) for the fields employed in this experiment. Since these ENDOR transitions are observed from ODMR peaks at different fields, an ENDOR frequency change due to the change in nuclear Larmor frequency is expected. Depending on the relative signs of the central hyperfine constants, the nearest-neighbor hyperfine constants, and the nuclear Larmor interactions, these frequency changes may either add or subtract. Our analysis shows that the central hyperfine constant and the nearest-neighbor hyperfine constants must have the same sign in order to explain the observed frequency shift.

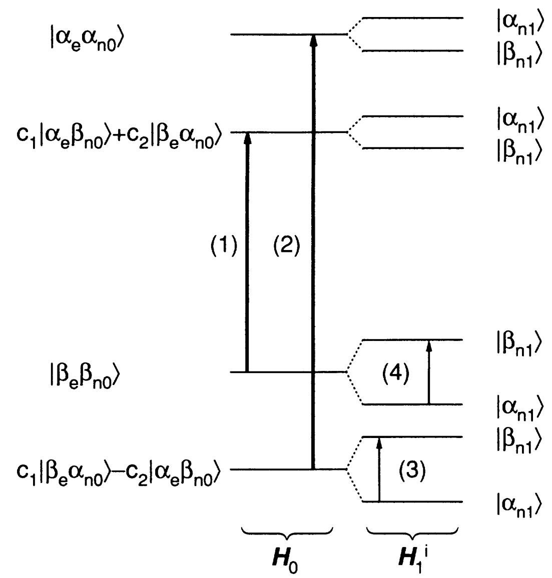

FIG. 3. Energy-level diagram for an $S=\frac{1}{2}$, $I_0=\frac{1}{2}$, $I_1=\frac{1}{2}$ spin system. The product Zeeman states for the electron and central nuclear spin are mixed by the large central hyperfine interaction. The coefficients c_1 and c_2, obtained by diagonalizing $\hat{\mathcal{H}}_0$, are 0.997 86 and 0.065 45 at 810 mT.

Although samples from different sources were used in our PL-ODENDOR experiments and Jeon's MCD-ODENDOR work, the samples are quite similar. The differences between the hyperfine parameters determined from the PL-ODENDOR, and the hyperfine parameters reported in the MCD-ODENDOR of Jeon *et al.* are more likely due to a difference in the analysis employed than to a difference in the defect observed. If the mixing effects of the central hyperfine interaction are neglected, our ENDOR data from the high-field ODMR line can be fitted reasonably well with the parameters reported by Jeon *et al.* To obtain a good fit to the ENDOR data from the low-field line, the parameters must be modified. When the central hyperfine effects are included in the analysis, ENDOR data from both the low-field and high-field lines can be fitted well with a single set of ligand hyperfine parameters. Clearly, the values determined for the ligand hyperfine parameters depend on the completeness of the model employed in the analysis, and whether fits of ENDOR data from both the ODMR lines are considered.

Another similarity between the PL-ODENDOR and the MCD-ODENDOR is the observation that ENDOR transitions originating from only one of the electron-spin manifolds were detected. Jeon *et al.* suggested that nuclear-spin polarization effects are responsible.[2] However, we have not been able to formulate an explanation along those lines for the PL-ODENDOR results. Another possible explanation involves thermalization among the excited DAP spin states. Luminescence-enhancing ENDOR signals result from inducing transitions between nuclear-spin sublevels of the long-lived DAP states. Furthermore, ENDOR transitions from the two electron-spin manifolds come from different long-lived DAP states, which may differ in population or lifetimes. Papers by Robins, Taylor, and Kennedy[10] and Viohl, Ohlsen, and Taylor[13] present evidence for a model of the P_{In} antisite ODMR process, in which the acceptor-bound hole spins are thermalized. The thermalized hole states lead to different recombination rates for the two electron-spin states. In the absence of microwaves, and if the electron-spin lattice relaxation is slow compared to recombination, this difference in recombination rates manifests itself in a population difference between the electron-spin states where the spin state with the longer recombination time is more populated. Nevertheless, the expected difference in recombination times and populations is insufficient to explain the absence of ENDOR transitions from one of the electron manifolds as simply due to a rapidly recombining or unpopulated electron-spin state. However, preliminary experimental evidence indicates that the observation of the PL-ODENDOR signals is closely connected to the transient portion of the ODMR response. Perhaps the observation of ENDOR signals from only one electron-spin manifold is related to the net transfer of electron spin from the less-populated state to the more-populated state, which gives rise to the transient response. As yet, the lack of ENDOR from the other electron-spin manifold has not been fully explained. This problem warrants further investigation, because it may provide insight into the mechanism of the ODENDOR response.

As Spaeth has pointed out, magnetic resonance detected through DAP luminescence may be severely broadened due to exchange interactions.[9] One way of overcoming this difficulty is to use a pulsed, time-resolved technique to obtain selectively ODMR from distant pairs which only experience a weak exchange interaction.[6,14] However, reducing the microwave modulation frequency in an ODMR experiment with continuous illumination also enhances the relative contribution to the ODMR from distant pairs.[15] PL-ODENDOR lines will also be affected by the exchange interaction. The ENDOR transitions for close pairs may be significantly broadened. However, since the magnitude of the exchange interaction falls off rapidly with increased pair separation, the ENDOR transitions for distant pairs will be largely unaffected. Thus, the modulation frequency dependence observed for the ^{31}P ENDOR lines suggests that the ENDOR signals detected at lower modulation frequencies are the sharper transitions from distant pairs. Since lowering the modulation frequency increases the contribution from distant pairs, it also increases the ENDOR signal.

The PL-ODENDOR peaks are in fact broader than the reported MCD-ODENDOR linewidths (1.2 vs 0.5 MHz). The PL-ODENDOR could indeed be broadened by the DAP exchange interaction. However, the exchange broadening of the ENDOR will be considerably smaller than the exchange broadening of the ODMR, because the effect of the exchange interaction on ENDOR frequencies is less direct. An appreciable isotropic exchange interaction will mix the electron-spin states in a manner analogous to the mixing produced by the large central hyperfine interaction. This mixing will produce a small shift in the ENDOR transition frequencies, just as the central hyperfine term does. Unlike the central hyperfine term, the magnitude of the exchange interaction is strongly dependent on DAP separation. The resulting range in magnitude of the exchange interaction creates a range of ENDOR frequency shifts, consequently broadening the ENDOR lines. Unfortunately, attempts to make this argument quantitative have not been successful. For an isotropic exchange interaction, the magnitude of the exchange term would have to vary over at least 1 GHz to account for the observed ENDOR linewidths. Although the ODMR linewidth is approximately 1 GHz, most of the linewidth can be accounted for as unresolved hyperfine splittings from the first ^{31}P shell. Given that the ODMR linewidth can be explained by mechanisms other than exchange broadening, and that the experimental conditions emphasize distant DAP's, it seems unlikely that the range of exchange interactions is large enough to explain the ENDOR linewidth. Perhaps a smaller but anisotropic exchange interaction could account for both the ENDOR and ODMR linewidths. We have not worked out the details for this case, but we would expect the ENDOR linewidths to be anisotropic. Actually, the ODENDOR lines are only slightly anisotropic. Therefore, accounting for the ENDOR linewidths with an anisotropic exchange mechanism seems unlikely.

In summary, the PL-ODENDOR of the ^{31}P nearest-neighbor shell for the P_{In} site in InP:Zn illustrates that well-resolved spectra can be obtained in spite of possible line broadening due to donor-acceptor exchange interactions. The PL-ODENDOR spectra are best when low microwave modulation frequencies are employed. This behavior may prove to be characteristic of all ENDOR detected via luminescence from DAP recombination when a range of pair separations exists. The defect observed is probably the same defect seen by the MCD-ODENDOR technique.

ACKNOWLEDGMENTS

We would like to thank J. R. Niklas, J.-M. Spaeth, F. C. Rong, and G. D. Watkins for discussions helpful in our ODENDOR spectrometer development. This work was supported in part by the Office of Naval Research. This work was done while one of us (H.C.C.) was at the Naval Research Laboratory with financial support from the National Research Council.

[1]D. M. Hoffman, B. K. Meyer, F. Lohse, and J.-M. Spaeth, Phys. Rev. Lett. **53**, 1187 (1984).

[2]D. Y. Jeon, H. P. Gislason, J. F. Donegan, and G. D. Watkins, Phys. Rev. B **36**, 1324 (1987).

[3]D. Y. Jeon, J. F. Donegan, and G. D. Watkins, Phys. Rev. B **39**, 3207 (1989).

[4]J. F. Donegan, D. Y. Jeon, and G. D. Watkins, Phys. Rev. B **43**, 2141 (1991).

[5]F. C. Rong, H. J. Sun, and G. D. Watkins, Phys. Rev. B **43**, 9108 (1991).

[6]D. Block, A. Hervé, and R. T. Cox, Phys. Rev. B **25**, 6049 (1982).

[7]J. J. Davies, J. E. Nicholls, and R. P. Barnard, J. Phys. C **18**, L93 (1985).

[8]H. P. Gislason, H. Sun, F. Rong, and G. D. Watkins, in *The 20th International Conference on the Physics of Semiconductors,* edited by E. M. Anastassakis and J. D. Joannopoulos (World Scientific, Singapore, 1990), p. 666.

[9]J. M. Spaeth, in *Proceedings of the 14th International Conference on Defects in Semiconductors,* edited by H. J. von Bardeleben (Trans Tech, Aedermannsdorf, 1986), p. 505.

[10]L. H. Robins, P. C. Taylor, and T. A. Kennedy, Phys. Rev. B **38**, 13 227 (1988).

[11]T. A. Kennedy and N. D. Wilsey, J. Cryst. Growth **83**, 198 (1987).

[12]D. Y. Jeon, Ph.D. thesis, Lehigh University, 1988.

[13]I. Viohl, W. D. Ohlsen, and P. C. Taylor, Phys. Rev. B **44**, 7975 (1991).

[14]D. Block and R. T. Cox, J. Lumin. **24/25**, 167 (1981).

[15]M. Godlewski and B. Monemar, J. Appl. Phys. **64**, 200 (1988).